

Robust Design Optimization of Electrical Machines Considering Hybrid Random and Interval Uncertainties

Bo Ma, Jing Zheng, Jianguo Zhu, Jinglai Wu, Gang Lei, and Youguang Guo

Abstract— In robust design optimization (RDO) of electrical machines, the cases with random uncertainty and interval uncertainty are generally investigated separately. The uncertainty quantification is based on the random method and interval method, respectively. For problems with hybrid uncertainties, the uncertainty analysis methods for a single type of uncertainties may no longer be applicable as both the random and interval methods are required for the uncertainty qualification. This poses considerable challenges to the hybrid uncertainty modeling, numerical calculation, and design optimization. This paper proposes an efficient robust optimizer based on the evolutionary algorithms and the polynomial chaos Chebyshev interval (PCCI) method for RDO of electrical machines with hybrid uncertainties. With the potential candidate filtering in the population of each iteration and effective robustness assessment by the PCCI method, the optimization can be conducted efficiently. A design example of a brushless DC motor considering hybrid uncertainties is analyzed and optimized. The results confirm the feasibility of the proposed method.

Index Terms— Robust design optimization, electrical machines, random-interval hybrid uncertainty, evolutionary algorithms, PCCI.

I. INTRODUCTION

In practical design optimization of electrical machines, uncertainties widely exist in the design dimensions, material properties, operation environment, and so on. The deterministic optimization method ignores the uncertainties, and aggressively optimizes the parameters for the best objectives. The optimal design obtained without robustness assessment may have a risk of high performance-diversity and faults [1, 2]. A robust design should be insensitive to the unavoidable tolerances and satisfy the reliability requirements [3, 4]. As an example, Fig. 1 illustrates a one-dimensional problem, where the dash lines are used to demonstrate the fluctuation intervals of points A and B. As shown, point A is the minimum objective. However, the sharp variation of the objective value in the uncertain interval means high-performance diversity of the same nominal design, which should be avoided in the design. On the other hand, the suboptimal point B shows a lower performance fluctuation or

higher robustness to uncertainties. How to obtain efficiently the optimal design with both high performance and reliability becomes a strong motivation to develop new effective robust optimization approaches taking into account the uncertainties.

For uncertain parameters with sufficient data points, e.g. dimension parameters of a product in mass production, they can be described by a specific probabilistic distribution. Under this condition, random methods can be applied to evaluate the robustness by the probabilistic properties such as the mean and variance of the structural performance. In some circumstance, the uncertain parameters can only be described by their interval bounds since there are not enough samples for achieving the probability distributions. For example, in the early stage of a design process, the designers can hardly obtain the distributions of uncertain parameters, but the bound information such as the dimension tolerances may be available. In this case, the interval methods can be applied to calculate the upper and lower bounds of performance fluctuation, which reflect the extreme conditions. Then, the worst case is utilized as the indicator of robustness.

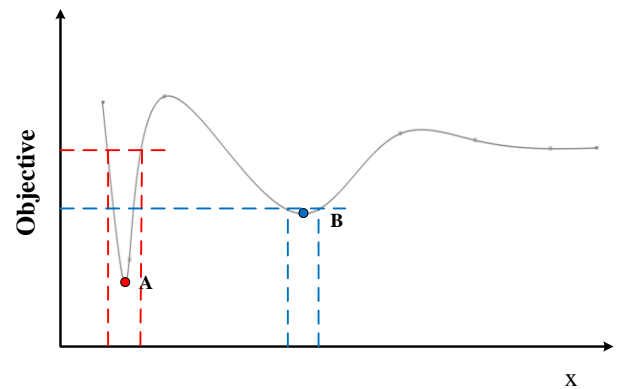


Fig. 1. Schematic diagram of the optimization problem with uncertainty.

The classical uncertainty quantification methods for problems with one type of uncertainties, such as the scanning approach (scanning the samples within the variation interval to determine the performance variation range) for the interval

Bo Ma, Gang Lei, Youguang Guo are with the School of Electrical and Data Engineering, University of Technology, Sydney, NSW 2007, Australia (e-mail: bo.ma@student.uts.edu.au; gang.lei@uts.edu.au; youguang.guo-1@uts.edu.au;).

Jing Zheng is with School of Mechanical and Vehicle Engineering, Hunan University, Changsha, Hunan Province, 410082, China (e-mail: jingzheng@hnu.edu.cn).

Jianguo Zhu is with School of Electrical and Information Engineering, University of Sydney, NSW 2007, Australia (e-mail: jianguo.zhu@sydney.edu.au).

Jinglai Wu is with School of Automotive and Transportation Engineering, Hefei University of Technology, Hefei 230009, China (e-mail: wjlhust@163.com).

uncertainty and the Monte Carlo method for the random uncertainty, are frequently used for performance perturbation quantification. Due to the large number of sampling points, the computation burden is heavy, especially for time-consuming models. For the robust optimization of electrical machines, the calculation cost would increase further due to the required large design population and optimization iterations to apply the intelligent algorithms [5, 6]. To handle the uncertainty quantification efficiently, various methods have been proposed, such as the polynomial chaos expansion method for the stochastic uncertainty [7, 8], the Taylor extension and Chebyshev expansion for interval uncertainty [9, 10], and the convergence accelerating techniques of optimization algorithms [11].

However, the scenario with both random and interval variables in the robust electrical machine optimization is rarely investigated. The above-mentioned approaches applied in the situation of a single type of uncertainty cannot estimate the reliability properly for problems with both random and interval uncertainties [12]-[14]. The computational burden is extremely heavy if the scanning and Monte Carlo approach (SMCA) is applied sequentially for the hybrid uncertainty analysis. Hence, some hybrid uncertainty qualification methods based on orthogonal polynomials have been proposed and proved to be very efficient for the uncertainty analysis. In this work, a robust optimizer based on the PCCI method and evolutionary algorithms is proposed for the robust optimization of electrical machines with hybrid uncertainties. In this optimizer, the PCCI method is applied to replace the SMCA for fast uncertainty quantification. For the intelligent algorithms of huge population and iteration amount, the filtering with deterministic constraints is proposed to reduce the individuals in each that require robustness analysis in each iteration and accelerate the optimization further.

In this paper, Section II introduces the classification of optimization models with different uncertainties, the theory of PCCI method, and the optimization framework. Section III presents a benchmark design example of a brushless DC motor, and Section IV the optimization results and a discussion of the mono-objective and multi-objective problems. Finally, Section V draws the conclusions.

II. ROBUST OPTIMIZATION WITH PCCI

A. Robust optimization model with uncertainties

In the deterministic optimization, the model usually can be defined as

$$\begin{aligned} \min : & f = f(\mathbf{d}) \\ \text{s.t. } & \mathbf{g}_k(\mathbf{d}) \leq 0, \\ & k = 1, 2, \dots, q \end{aligned} \quad (1)$$

where \mathbf{d} is a vector of design variables, $f(\mathbf{d})$ the objective function, and $\mathbf{g}_k(\mathbf{d})$ the k th constraint.

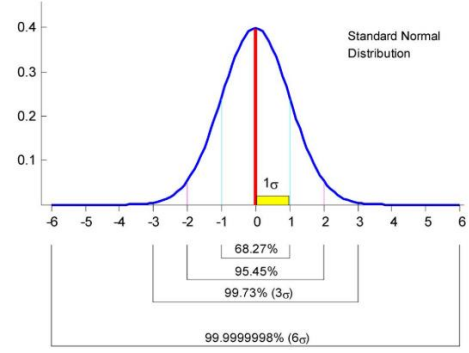


Fig. 2. Sigma level and its equivalent probability for the standard normal distribution.

In the robust optimization, considering the uncertainties, the problem can be defined as

$$\begin{aligned} \min : & f(\mathbf{d}, \boldsymbol{\zeta}) \\ \text{s.t. } & \mathbf{g}_k(\mathbf{d}, \boldsymbol{\zeta}) \leq 0, \\ & k = 1, 2, \dots, q \end{aligned} \quad (2)$$

where $\boldsymbol{\zeta}$ is a vector of independent uncertainty variables, and the design variables, \mathbf{d} , can have uncertainties as well.

When there exist only the random uncertainties, the robust optimization model can be described as

$$\begin{aligned} \min : & \mu[f(\mathbf{d}, \mathbf{X})] + n_f \sigma[f(\mathbf{d}, \mathbf{X})] \\ \text{s.t. } & \mu[\mathbf{g}_k(\mathbf{d}, \mathbf{X})] + n_g \sigma[\mathbf{g}_k(\mathbf{d}, \mathbf{X})] \leq 0, \\ & k = 1, 2, \dots, q \\ & \mathbf{X} \square N(\boldsymbol{\mu}_x, \boldsymbol{\sigma}_x^2) \end{aligned} \quad (3)$$

where \mathbf{X} is the random uncertainty vector, n_f the weighting factor for the diversity of objectives, n_g is the sigma level, and μ and σ are the calculated mean and standard deviation, respectively.

For robust design optimization problems, the design for six sigma (DFSS) approach is commonly used, i.e. by setting the factor $n_g=6$ [15, 16]. Fig. 2 illustrates the sigma level and its equivalent probability for the standard normal distribution. In the case of DFSS optimization, a large probability of the product in mass production can be promised without violating the constraints.

When there exist only the interval uncertainties, the robust optimization is modeled by the worst case, i.e. the upper bounds of the objective function and constraints expressed as

$$\begin{aligned} \min : & \max f(\mathbf{d}, \mathbf{Y}) \\ \text{s.t. } & \max \mathbf{g}_k(\mathbf{d}, \mathbf{Y}) \leq 0, \\ & k = 1, 2, \dots, q \\ & \boldsymbol{\lambda} - \boldsymbol{\delta} \leq \mathbf{Y} \leq \boldsymbol{\lambda} + \boldsymbol{\delta} \end{aligned} \quad (4)$$

where \mathbf{Y} is the interval uncertainty vector with nominal $\boldsymbol{\lambda}$ and bound $\boldsymbol{\delta}$.

In the case of the hybrid uncertainties, the objective functions and constraints have the characteristics of both the random and interval uncertainties. The robust optimization considering the

hybrid uncertainties can then be expressed as

$$\begin{aligned} \min : & \max \left\{ \mu[f(\mathbf{d}, \mathbf{X}, \mathbf{Y})] + n_f \sigma[f(\mathbf{d}, \mathbf{X}, \mathbf{Y})] \right\} \\ \text{s.t.} : & \max \left\{ \mu[g_k(\mathbf{d}, \mathbf{X}, \mathbf{Y})] + n_g \sigma[g_k(\mathbf{d}, \mathbf{X}, \mathbf{Y})] \right\} \leq 0, \\ & k = 1, 2, \dots, q \\ & \mathbf{X} \square N(\boldsymbol{\mu}_x, \boldsymbol{\sigma}_x^2) \\ & \boldsymbol{\lambda} - \boldsymbol{\delta} \leq \mathbf{Y} \leq \boldsymbol{\lambda} + \boldsymbol{\delta} \end{aligned} \quad (5)$$

To estimate the extreme values of objectives and constraints, the mean and standard deviation are calculated separately as illustrated in Fig. 3. Then, the worst-case under this situation can be estimated as the sum of the upper bounds of mean and standard deviation multiplied by the sigma level factor, and (5) can be rewritten as

$$\begin{aligned} \min : & \mu_{ub}[f(\mathbf{d}, \mathbf{X}, \mathbf{Y})] + n_f \sigma_{ub}[f(\mathbf{d}, \mathbf{X}, \mathbf{Y})] \\ \text{s.t.} : & \mu_{ub}[g_k(\mathbf{d}, \mathbf{X}, \mathbf{Y})] + n_g \sigma_{ub}[g_k(\mathbf{d}, \mathbf{X}, \mathbf{Y})] \leq 0, \\ & k = 1, 2, \dots, q \\ & \mathbf{X} \square N(\boldsymbol{\mu}_x, \boldsymbol{\sigma}_x^2) \\ & \boldsymbol{\lambda} - \boldsymbol{\delta} \leq \mathbf{Y} \leq \boldsymbol{\lambda} + \boldsymbol{\delta} \end{aligned} \quad (6)$$

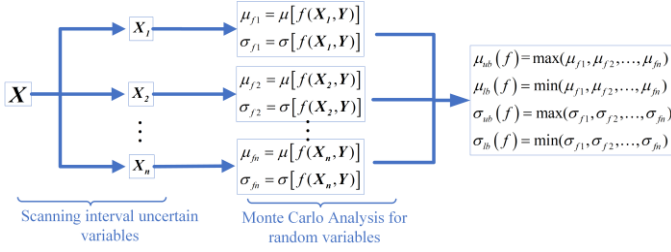


Fig. 3. Estimation process of extreme values of mean and standard deviation for a problem with hybrid uncertainty.

B. Uncertainty analysis based on the PCCI method

This section introduces the PCCI method [17] in which the random uncertainties are accounted for by the polynomial chaos (PC) method and the interval uncertainties are quantified by the Chebyshev interval (CI) functions.

The random and interval uncertainty vectors are noted as \mathbf{X} and \mathbf{Y} in a performance function $P(\mathbf{X}, \mathbf{Y})$. If the uncertainty variables are non-standard, they should be firstly transformed into the standard normal variables, ξ_i ($i=1, 2, \dots, n$), that belongs to $N(0, 1)$ and the standard interval variables, η_j ($j=1, 2, \dots, m$), that belongs to $[-1, 1]$. For convenience without losing any generality, the uncertainty variables are assumed as standard.

As the first step, by considering only the random uncertainty parameters, the performance function $P(\boldsymbol{\xi}, \boldsymbol{\eta})$ can be expanded by the p th order polynomial as the following

$$P(\boldsymbol{\xi}, \boldsymbol{\eta}) = \sum_{\boldsymbol{\chi} \in \mathbb{N}^n, \|\boldsymbol{\chi}\| \leq p} c_{\boldsymbol{\chi}}(\boldsymbol{\eta}) H_{\boldsymbol{\chi}}(\boldsymbol{\xi}) \quad (7)$$

where $\boldsymbol{\chi}$ is the index vector $(\chi_1, \chi_2, \dots, \chi_n)$ while

$$\begin{aligned} \chi_i &= 0, 1, \dots, p \\ i &= 1, 2, \dots, m \end{aligned} \quad (8)$$

$$\|\boldsymbol{\chi}\| = \chi_1 + \chi_2 + \dots + \chi_n \quad (9)$$

According to this condition, the term number, i.e. the coefficient number can be obtained as

$$k = C_{n+p}^p \quad (10)$$

$H_{\boldsymbol{\chi}}(\boldsymbol{\xi})$ and $c_{\boldsymbol{\chi}}(\boldsymbol{\eta})$ ($\boldsymbol{\chi} \in \mathbb{N}^n$ and $\|\boldsymbol{\chi}\| \leq p$) are the multivariate Hermite polynomial and coefficients, respectively, and $c_{\boldsymbol{\chi}}(\boldsymbol{\eta})$ can be obtained by the least square method as

$$c_{\boldsymbol{\chi}}(\boldsymbol{\eta}) = (\mathbf{A}^T \mathbf{A})^{-1} \mathbf{A}^T \mathbf{P}(\boldsymbol{\xi}, \boldsymbol{\eta}) \quad (11)$$

$$\mathbf{A} = \begin{bmatrix} H_{\boldsymbol{\chi}^{(1)}}(\boldsymbol{\xi}^{(1)}) & H_{\boldsymbol{\chi}^{(2)}}(\boldsymbol{\xi}^{(1)}) & \dots & H_{\boldsymbol{\chi}^{(k)}}(\boldsymbol{\xi}^{(1)}) \\ H_{\boldsymbol{\chi}^{(1)}}(\boldsymbol{\xi}^{(2)}) & H_{\boldsymbol{\chi}^{(2)}}(\boldsymbol{\xi}^{(2)}) & \dots & H_{\boldsymbol{\chi}^{(k)}}(\boldsymbol{\xi}^{(2)}) \\ \vdots & \vdots & \ddots & \vdots \\ H_{\boldsymbol{\chi}^{(1)}}(\boldsymbol{\xi}^{(l)}) & H_{\boldsymbol{\chi}^{(2)}}(\boldsymbol{\xi}^{(l)}) & \dots & H_{\boldsymbol{\chi}^{(k)}}(\boldsymbol{\xi}^{(l)}) \end{bmatrix} \quad (12)$$

k is the number of terms in (7), and l denotes the number of samples for the random variables.

From (7), the performance function with hybrid random and interval uncertainties can be expressed by the coefficients, which are functions of the interval uncertainties, and the multivariate polynomials, which are functions of the random variables. The intervals are regarded as fixed values.

The second step takes into account the interval uncertainties. By the p th order Chebyshev inclusion function, the interval coefficient can be approximated as

$$c_{\boldsymbol{\chi}}(\boldsymbol{\eta}) = \sum_{\boldsymbol{\gamma} \in \mathbb{N}^m, \|\boldsymbol{\gamma}\| \leq p} c_{\boldsymbol{\chi}, \boldsymbol{\gamma}} \Psi_{\boldsymbol{\gamma}}(\boldsymbol{\eta}) \quad (13)$$

where $\boldsymbol{\gamma}$ is a vector of multiple indices consisting of

$$\begin{aligned} \gamma_j &= 0, 1, \dots, p \\ j &= 1, 2, \dots, m \end{aligned} \quad (14)$$

indicating the components of the multivariate Chebyshev polynomial, $c_{\boldsymbol{\chi}, \boldsymbol{\gamma}}$ are the coefficients, and

$$\Psi_{\boldsymbol{\gamma}}(\boldsymbol{\eta}) = \prod_{j=1}^m \varphi_{\gamma_j}(\eta_j) \quad (15)$$

is the multivariate Chebyshev polynomial built from the univariate polynomial

$$\varphi_{\gamma_j}(\eta_j) = \cos(\gamma_j [\theta_j]) \quad (16)$$

$$[\theta_j] = \arccos(\eta_j) = [0, \pi] \quad (17)$$

Similar to (9) and (10), the coefficients $c_{\boldsymbol{\chi}, \boldsymbol{\gamma}}$ can be obtained by the least square method.

In the above analysis, (7) and (11) can be considered in one framework, termed as the PCCI method, and the coefficients $c_{\boldsymbol{\chi}, \boldsymbol{\gamma}}$ as the PCCI expansion coefficients. The performance function with hybrid uncertainties can be approximated by

$$P(\boldsymbol{\xi}, \boldsymbol{\eta}) = \sum_{\boldsymbol{\chi} \in \mathbb{N}^n} \sum_{\boldsymbol{\gamma} \in \mathbb{N}^m} c_{\boldsymbol{\chi}, \boldsymbol{\gamma}} \Psi_{\boldsymbol{\gamma}}(\boldsymbol{\eta}) H_{\boldsymbol{\chi}}(\boldsymbol{\xi}) \quad (18)$$

and the PCCI expansion coefficients can be calculated by using the least square method twice as

$$\mathbf{c}_{\mathbf{x},\boldsymbol{\gamma}} = (\mathbf{B}^T \mathbf{B})^{-1} \mathbf{B}^T \mathbf{P}^T \mathbf{A} (\mathbf{A} \mathbf{A}^T)^{-1} \quad (19)$$

where \mathbf{A} and \mathbf{B} are the sample matrices with components $A_{rs} = H_{\chi^{(s)}}(\xi^{(r)})$, $B_{rs} = \Psi_{\gamma^{(s)}}(\eta^{(r)})$, and $\xi^{(r)}$ and $\eta^{(r)}$ the collocation points of random and interval variables selected from the zeros of the one dimensional higher Hermite polynomials and Chebyshev polynomials, respectively. $P(\xi, \eta)$ is the output vector at the collocation points. In order to ensure the numerical stability, the number of sampling points is recommended to twice the number of coefficients for obtaining a robust estimation.

Finally, based on the orthonormal properties of the polynomials, the mean and interval variance of the performance function can be obtained by

$$\mu(P(\xi, \eta)) = \sum_{\gamma \in \mathbb{N}^m, \|\boldsymbol{\gamma}\| \leq p} c_{0,\gamma} \Psi_{\gamma}(\boldsymbol{\eta}) \quad (20)$$

$$\sigma^2(P(\xi, \eta)) = \sum_{\chi \in \mathbb{N}^n, \chi \neq 0, \|\boldsymbol{\chi}\| \leq p} \left(\sum_{\gamma \in \mathbb{N}^m, \|\boldsymbol{\gamma}\| \leq p} c_{\chi,\gamma} \Psi_{\gamma}(\boldsymbol{\eta}) \right)^2 \quad (21)$$

The mean and variance in (18) and (19) are functions of the interval uncertainties, and they have intervals with lower and upper bounds. Based on the characteristics of the trigonometric functions, we know that $\Psi_0(\boldsymbol{\eta}) = 0$ and $\Psi_{\gamma \in \mathbb{N}^m, \gamma \neq 0}(\boldsymbol{\eta}) = [-1, 1]$.

The bounds of the mean and standard variance can thus be easily approximated, as the following

$$\mu(f(\xi, \eta)) = \left[\begin{array}{c} c_{0,0} - \left(\sum_{\gamma \in \mathbb{N}^m, \gamma \neq 0, \|\boldsymbol{\gamma}\| \leq p} |c_{0,\gamma}| \right) \\ c_{0,0} + \left(\sum_{\gamma \in \mathbb{N}^m, \gamma \neq 0, \|\boldsymbol{\gamma}\| \leq p} |c_{0,\gamma}| \right) \end{array} \right] \quad (22)$$

$$\sigma(P(\xi, \eta)) = \left[\begin{array}{c} \sqrt{\sum_{\chi \in \mathbb{N}^n, \chi \neq 0, \|\boldsymbol{\chi}\| \leq p} \sum_{\gamma \in \mathbb{N}^m, \|\boldsymbol{\gamma}\| \leq p} c_{\chi,\gamma}^2 - 2 \sum_{\chi \in \mathbb{N}^n, \chi \neq 0, \|\boldsymbol{\chi}\| \leq p} \sum_{\gamma \in \mathbb{N}^m, \|\boldsymbol{\gamma}\| \leq p} c_{\chi,\gamma^{(k_1)}} c_{\chi,\gamma^{(k_2)}}} \\ \sqrt{\sum_{\chi \in \mathbb{N}^n, \chi \neq 0, \|\boldsymbol{\chi}\| \leq p} \sum_{\gamma \in \mathbb{N}^m, \|\boldsymbol{\gamma}\| \leq p} c_{\chi,\gamma}^2 + 2 \sum_{\chi \in \mathbb{N}^n, \chi \neq 0, \|\boldsymbol{\chi}\| \leq p} \sum_{\gamma \in \mathbb{N}^m, \|\boldsymbol{\gamma}\| \leq p} c_{\chi,\gamma^{(k_1)}} c_{\chi,\gamma^{(k_2)}}} \end{array} \right] \quad (23)$$

where $\gamma^{(k_1)}$ and $\gamma^{(k_2)}$ are two realizations of the index γ . These two equations provide two efficient and convenient approximations for the interval bounds. Since all the Chebyshev polynomials are not possible to achieve -1 or 1 at the same time, the estimations by (20) and (21) inevitably involve overestimations. Proper algorithms, e.g. the scanning method, can be used to better control the overestimation and obtain the bounds of the interval mean and standard variance, as follows:

$$\mu(P(\xi, \eta)) = \left[\begin{array}{c} \min \sum_{\gamma \in \mathbb{N}^m, \|\boldsymbol{\gamma}\| \leq p} c_{0,\gamma} \Psi_{\gamma}(\boldsymbol{\eta}) \\ \max \sum_{\gamma \in \mathbb{N}^m, \|\boldsymbol{\gamma}\| \leq p} c_{0,\gamma} \Psi_{\gamma}(\boldsymbol{\eta}) \end{array} \right] \quad (24)$$

$$\sigma(P(\xi, \eta)) = \left[\begin{array}{c} \sqrt{\min \sum_{\chi \in \mathbb{N}^n, \chi \neq 0, \|\boldsymbol{\chi}\| \leq p} \left(\sum_{\gamma \in \mathbb{N}^m, \|\boldsymbol{\gamma}\| \leq p} c_{\chi,\gamma} \Psi_{\gamma}(\boldsymbol{\eta}) \right)^2} \\ \sqrt{\max \sum_{\chi \in \mathbb{N}^n, \chi \neq 0, \|\boldsymbol{\chi}\| \leq p} \left(\sum_{\gamma \in \mathbb{N}^m, \|\boldsymbol{\gamma}\| \leq p} c_{\chi,\gamma} \Psi_{\gamma}(\boldsymbol{\eta}) \right)^2} \end{array} \right] \quad (25)$$

C. Optimization framework

With the proposed hybrid uncertainty analysis approach and intelligent algorithms, the robust optimization flowchart is established as shown in Fig. 4. It mainly includes the following seven steps.

Step 1: Specify the design variables, uncertain parameter of the initial design, deterministic and robust objectives and constraints of the design optimization problem. Determine the algorithm parameters and stop criterion.

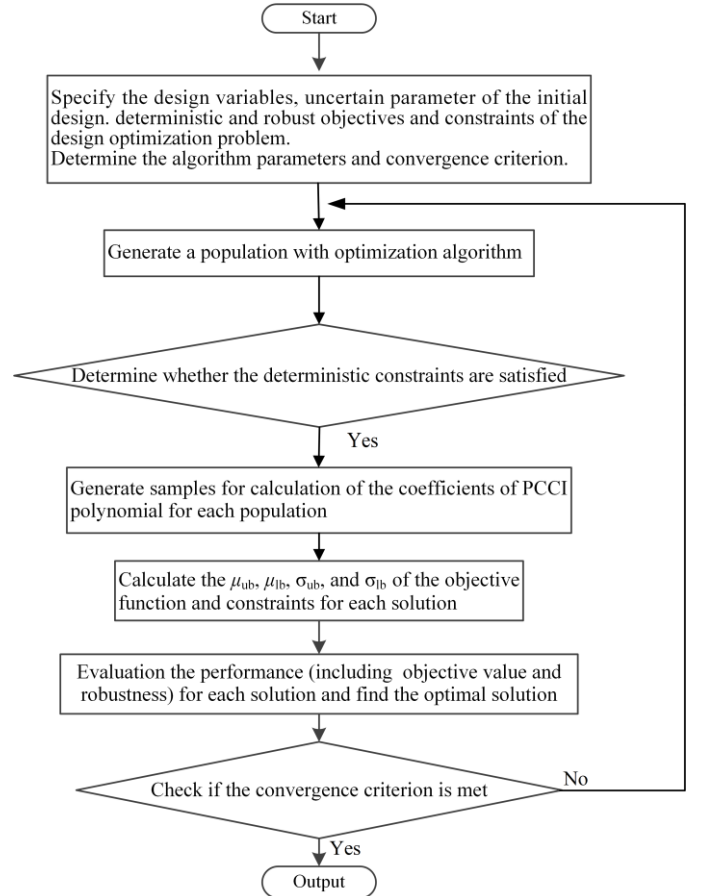


Fig. 4. Flowchart of the optimization approach.

- Step 2: Generate a population for the intelligent optimization algorithm.
- Step 3: If the solution in the population cannot meet the requirements of the deterministic constraints, there is no need for this solution to do the reliability analysis with the PCCI. Therefore, to accelerate the algorithm, the constraint of the population is evaluated in this step. Only if the constraints are satisfied, the reliability analysis is conducted in the following steps for the solution.
- Step 4: Generate samples according to the uncertain variables for the solution to calculate the coefficients of the PCCI model by the least square method.
- Step 5: Estimate the upper and lower bounds of the mean and standard deviation values for the objective function and constrains by the established PCCI model.
- Step 6: Evaluate the robustness of the solutions according to specified reliability settings.
- Step 7: Check the convergence of the current optimal solution. If the results meet the requirement of the iteration, output the design. Otherwise, go to step 2 to continue the iteration.

III. NUMERICAL EXAMPLE

To investigate the effectiveness of the proposed robust optimizer, a brushless DC wheel motor benchmark is selected as the design example [18]. The motor is designed for propelling a solar vehicle to meet the specifications of 20Nm torque at 721rpm while the maximal speed reached at no-load is specified also is 1442. The initial design is an outer rotor brushless DC motor with surface mounted magnets, concentrated windings, 18 slots and 12 poles. Fig. 5 shows the topology of the brushless DC motor.

As a design benchmark, the example shows characteristics in explicit equations, scaled design variables, and objectives, etc. As well, it includes highly constrained multidisciplinary and multimodal features. The analytical design model consists of 78 nonlinear equations of the electromagnetic and thermal performances.

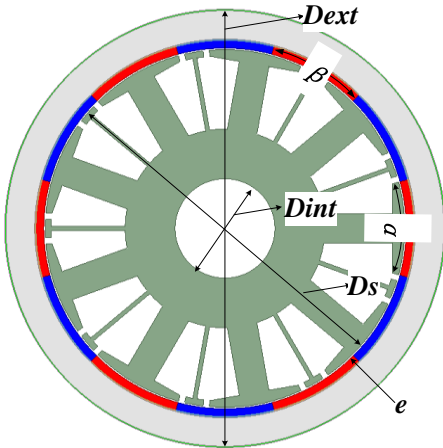


Fig. 5. Topology of the brushless DC motor.

The benchmark can be used for problems of both single and

multiple objectives. When it is optimized as a single objective problem to achieve the highest efficiency under certain technical constraints, it can be defined as

$$\begin{aligned} \max \quad & f_1 = \eta \\ \text{s.t.} \quad & \begin{cases} M_{\text{tot}} \leq 15\text{kg}, D_{\text{int}} \geq 76\text{mm}, I_{\text{max}} \geq 125\text{A} \\ D_{\text{ext}} \leq 340\text{mm}, T_a \leq 120^\circ\text{C}, \text{discr} \geq 0 \end{cases} \end{aligned} \quad (26)$$

where M_{tot} is the total mass of the motor, D_{ext} the external diameter of the motor, D_{int} the inner diameter of the stator, I_{max} the maximum demagnetization current, T_a the temperature of the magnets, and discr the determinant used for the calculation of slot height.

While sharing the same constraints, for multiple optimization objectives of the highest efficiency and the lowest total mass, the problem can be expressed as

$$\text{obj.} \quad \begin{cases} \max \quad f_1 = \eta \\ \min \quad f_2 = M_{\text{tot}} \end{cases} \quad (27)$$

The optimization problem contains five-design parameters, as listed in Table I. It is assumed that the two stochastic parameters obey the Gaussian distribution and the three interval parameters are hypothesized. Specifically, the design variable D_s also has random uncertain property. The uncertainty variables of the two uncertainty types and their properties are presented in Tables II and III below, respectively.

For this design example, the weighting factor n_f and sigma level n_g are set as 6. In order to prove the feasibility of the proposed optimizer, the deterministic and robust optimizations based on SMCA are also conducted. SMCA is also utilized to analyze the robustness of the optimization results. The robust optimization objectives can be expressed as

$$\begin{aligned} \min : \quad & F_1 = -[\mu_{ub}(\eta) + 6\sigma_{ub}(\eta)] \\ \min : \quad & F_2 = \mu_{ub}(M_{\text{tot}}) + 6\sigma_{ub}(M_{\text{tot}}) \end{aligned} \quad (28)$$

while the constraints share the same format as (6).

TABLE I
DESIGN PARAMETERS

Par.	Description	Unit	lower	upper
B_e	Maximum magnetic flux density in the air gap	T	0.5	0.76
B_d	Average magnetic flux density in the teeth	T	0.9	1.8
B_{es}	Average magnetic flux density in stator back iron	T	0.6	1.6
D_s	Stator outer diameter	mm	150	330
J	Current density	A/mm ²	2	5

TABLE II
PARAMETERS WITH INTERVAL UNCERTAINTY

Par.	Description	Unit	λ	δ
α	Width of stator tooth	deg.	30	0.08
e	Length of air gap	mm	0.8	0.02
β	Width of intermediate tooth	deg.	6	0.08

TABLE III

PARAMETERS WITH RANDOM UNCERTAINTY

Par.	Description	Unit	μ	σ
D_s	Stator outer diameter	mm	-	0.1
L_m	Length of the motor	mm	45	0.1

IV. RESULTS AND DISCUSSION

A. Optimization results of the single objective problem

Table IV lists the optimization results of the benchmark obtained by the deterministic and robust optimization methods with PCCI and SMCA. The two robust optimization approaches yield the same objective values, which are very close to those obtained by the deterministic design optimization approaches.

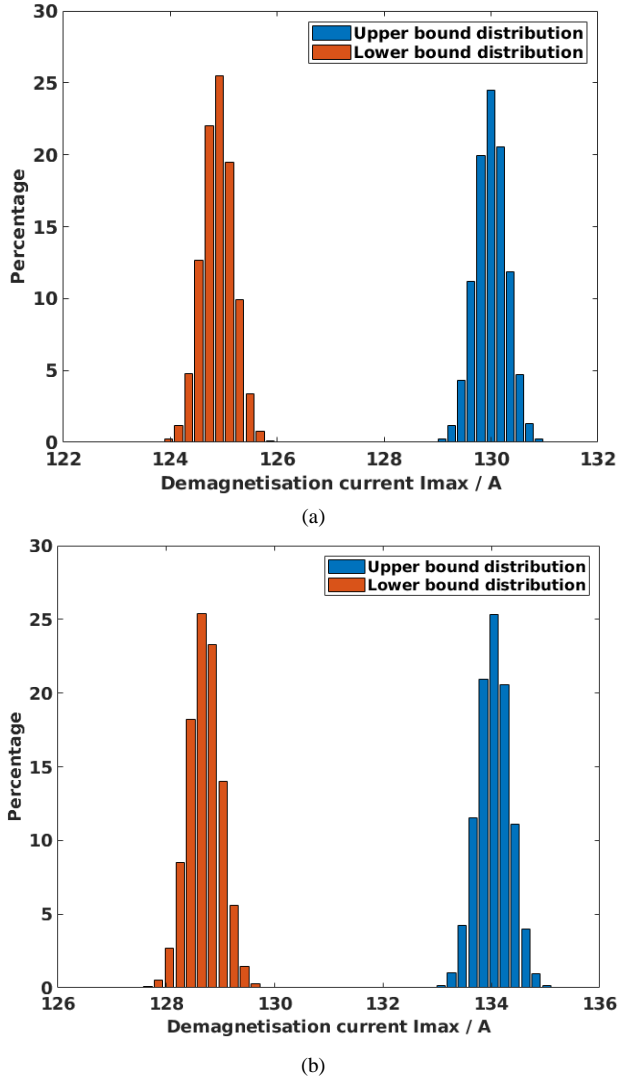
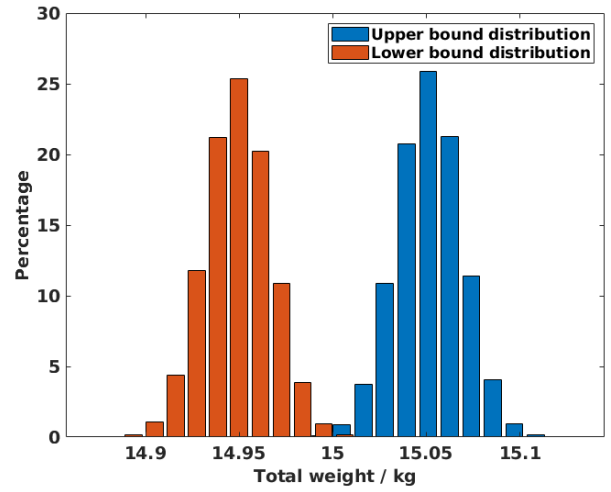
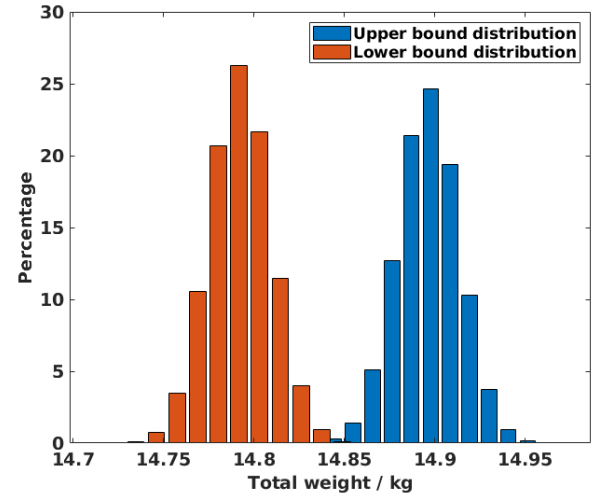


Fig. 6. Demagnetization current distribution: (a) deterministic solution, and (b) robust solution with PCCI.



(a)



(b)

Fig. 7. Total weight distribution: (a) deterministic solution, and (b) robust solution with PCCI.

TABLE IV
OPTIMAL DESIGN PARAMETERS AND OBJECTIVES

Par.	Unit	Deter	PCCI	SMCA
B_d	T	1.8	1.8	1.8
B_e	T	0.650	0.655	0.655
B_{cs}	T	0.950	0.975	0.99
D_s	mm	202.5	201.0	201.0
J	A/mm ²	2.0499	2.0736	2.0661
f_1		0.9531		
$-F_1$			0.9526	0.9526

TABLE V
UPPER BOUND MEAN VALUE OF THE PERFORMANCES

	Unit	SMCA	PCCI		
η		0.9530	0.9530	1.9560E-5	1.9438E-5
D_{int}	mm	80.80	80.82	3.7310E-1	3.6175E-1
D_{ext}	mm	239.3	239.0	1.2029E-1	1.1569E-1
$discr$		0.0252	0.0255	3.5492E-4	3.4305E-4

I_{max}	A	134.0420	132.5106	0.3012	0.2904
Ta	°C	95.6889	95.6889	0.0769	0.0751
M_{tot}	kg	14.8964	14.8776	0.0170	0.0167

TABLE VI
UPPER BOUND STANDARD DEVIATION OF THE PERFORMANCES

	Unit	SMCA	PCCI
η		1.9560E-5	1.9438E-5
D_{int}	mm	3.7310E-1	3.6175E-1
D_{ext}	mm	1.2029E-1	1.1569E-1
$discr$		3.5492E-4	3.4305E-4
I_{max}	A	0.3012	0.2904
Ta	°C	0.0769	0.0751
M_{tot}	kg	0.0170	0.0167

From the aspect of robustness, each solution is evaluated according to the maximum upper bounds of the mean and standard values obtained by SMCA. The verification results show that the sigma levels of the constraints are no less than the pre-set value of 6 for the PCCI solution. On the contrary, since there is no reliability assessor in the deterministic optimization, the robustness of the deterministic solution is not guaranteed. Particularly, the demagnetization current that the permanent magnets can tolerate should be larger than 125 A, while the total weight is limited no more than 15 kg. Figs. 6 and 7 illustrate the upper and lower bound distributions of the demagnetization current and weight for the deterministic and robust solutions with PCCI. The results show that the possibility of the deterministic solution violates the constraints, while the robustness of solution with PCCI is well promised.

To illustrate the accuracy of the PCCI method, Tables V and VI list the upper bounds of the mean and standard deviation of the performances included in the objective and constraints. The comparison results demonstrate the high precision of the PCCI approach in the estimation of robustness information. From the perspective of efficiency, for the interval and random parameters, the number of scanning and Monte Carlo sampling points is 1,000 respectively, which means that the number of total sampling points is 10^6 while only 60 samples are required for the second-order PCCI modeling. For the robustness estimation of one potential design, the SMCA takes 1.95 s while the PCCI method requires only 0.25 s, which is 7 times faster than the SMCA. Furthermore, the calling time of robustness assessment by PCCI method was reduced from 10^4 (iteration step \times population size i.e. 200×50) to 2073, which means the potential solutions required for the robustness calculation are decreased to about 20 percent for this case.

When the time-consuming model is utilized such as the finite element model, the merits of the PCCI will be more prominent.

B. Optimization Results of the Multi-objective Problem

Fig. 8 illustrates the Pareto diagram of the deterministic and robust optimizations. As shown, the robust solutions are more conservative than the deterministic solutions for achieving the optimal efficiency and total weight. Meanwhile, the robust solutions achieved by the two optimizers are close to each other,

confirming the accuracy of the proposed method.

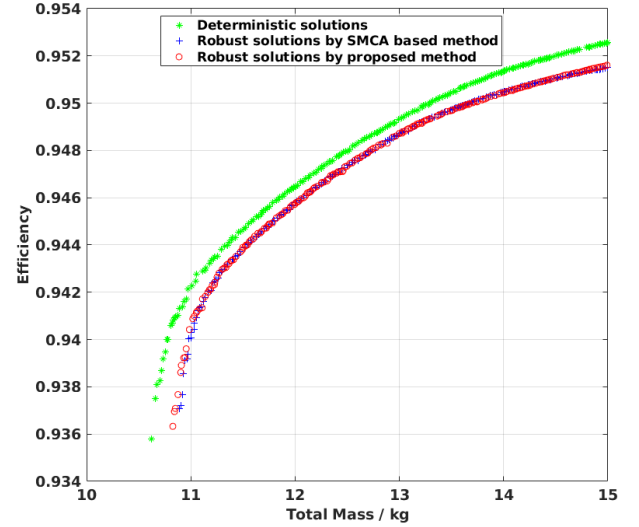


Fig. 8. Pareto diagram of the deterministic and robust optimizations.

As a further proof of the robustness of the solutions obtained by the PCCI optimizer, their sigma levels verified by the SMCA are present in Fig. 9. Particularly, the sigma level used is the minimum one among all constraints. In contrast to the deterministic solutions, the sigma levels of robust solutions are higher than the set value of 6.

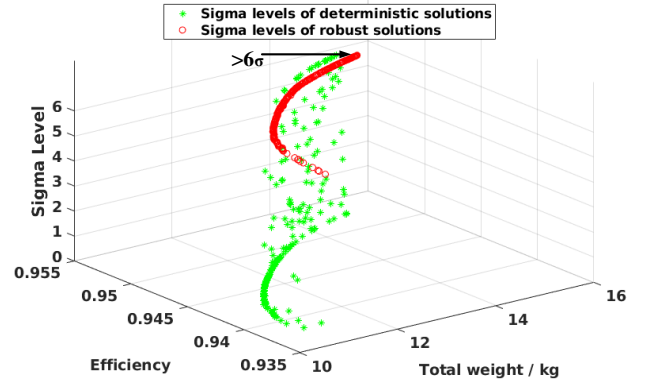
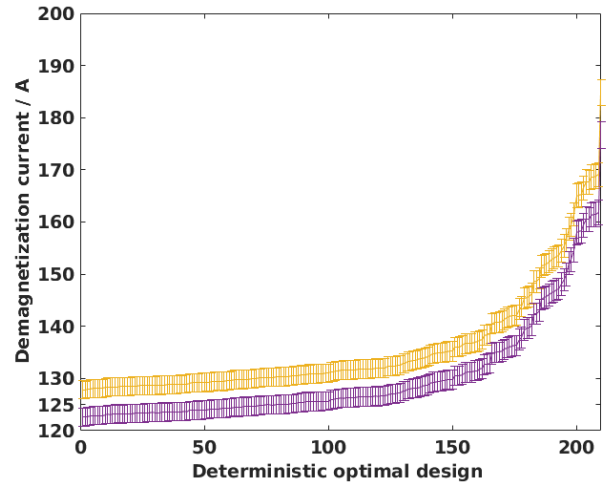


Fig. 9. Sigma level of the solutions.



(a)

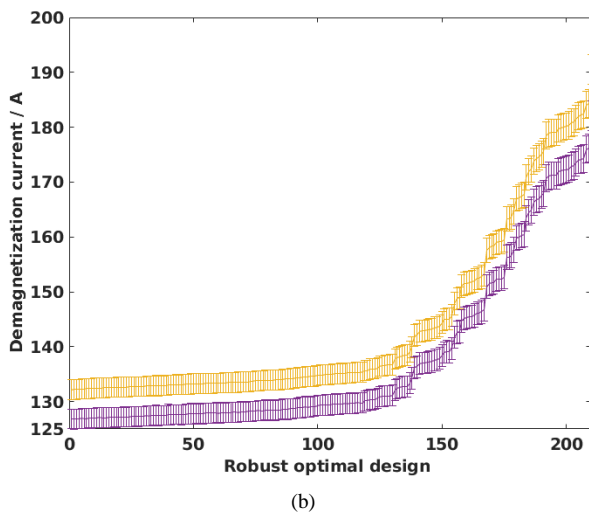


Fig. 10. Demagnetization current of the deterministic and robust solutions.

Fig. 10 shows the error bar diagrams of the demagnetization current of the solutions where the middle points of the yellow and purple bars are the upper- and lower-bound mean values, respectively. The lengths of each error bar above and below the mean values are $6\sigma_{ub}(I_{\max})$, i.e. six times the upper bound of demagnetization current standard deviation. The demagnetization current between the upper bound of the yellow bar and the lower bound of the purple bar are regarded as the performance value that the solution may have. As shown, various deterministic solutions violate the demagnetization current constraints, while the lower bounds of robust solutions are larger than 125 A.

V. CONCLUSION

The effectiveness and robustness of the proposed approach were confirmed by comparing with the deterministic optimization of a brushless DC motor benchmark design problem. Meanwhile, compared with the classical SMCA based robust optimization process, the optimization efficiency can be improved by using the PCCI method. The robustness verification of the solution obtained by the proposed approach with SMCA also shows the accuracy of PCCI in the uncertainty quantification. From the above analysis, the feasibility of the proposed optimization methodology was validated for robust optimization of electrical machines with hybrid uncertainties.

REFERENCES

- [1] G. Lei, J. Zhu, and Y. Guo, *Multidisciplinary Design Optimization Methods for Electrical Machines and Drive Systems*, Springer-Verlag Berlin Heidelberg, 2016.
- [2] J. G. Lee, N. W. Hwang, H. R. Ryu, H. K. Jung, and D. K. Woo, "Robust optimization approach applied to permanent magnet synchronous motor," *IEEE Trans. Magn.*, vol. 53, no. 6, pp. 1-4, Jun. 2017.
- [3] G. Lei, J. Zhu, Y. Guo, C. Liu, and B. Ma, "A review of design optimization methods for electrical machines," *Energies*, vol. 10, no. 12, Art. no. 1962, pp. 1-31, 2017.
- [4] S. Cho, J. Jang, S. Lee, *et al.*, "Reliability-based optimum tolerance design for industrial electromagnetic devices," *IEEE Trans. Magn.*, vol. 50, no. 2, pp. 713-716, Feb. 2014.
- [5] R. Storn and K. Price, "Differential evolution—A simple and efficient heuristic for global optimization over continuous spaces," *J. Glob. Optim.*, vol. 11, pp. 341-359, 1997.
- [6] G. C. Tenaglia and L. Lebensztajn, "A multiobjective approach of differential evolution optimization applied to electromagnetic problems," *IEEE Trans. Magn.*, vol. 50, no. 2, pp. 625-628, Feb. 2014.
- [7] D. Kim, B. Kang, K. K. Choi, and D. Kim, "A Comparative study on probabilistic optimization methods for electromagnetic design," *IEEE Trans. Magn.*, vol. 52, no. 3, pp. 1-4, Mar. 2016.
- [8] S. L. Ho and S. Yang, "A fast robust optimization methodology based on polynomial chaos and evolutionary algorithm for inverse problems," *IEEE Trans. Magn.*, vol. 48, no. 2, pp. 259-262, Feb. 2012.
- [9] J. L. Wu, Z. Luo, Y. Q. Zhang, N. Zhang, and L. P. Chen, "Interval uncertain method for multibody mechanical systems using Chebyshev inclusion functions," *Int. J. for Numerical Methods in Eng.*, vol. 95, no. 7, pp. 608-630, June 2013.
- [10] L. Egiziano, P. Lamberti, G. Spagnuolo, and V. Tucci, "Robust design of electromagnetic systems based on interval Taylor Extension applied to a multiquadratic performance function," *IEEE Trans. Magn.*, vol. 44, no. 6, pp. 1134-1137, June 2008.
- [11] S. L. Ho, S. Yang, Y. Bai, and Y. Li, "A wind driven optimization-based methodology for robust optimizations of electromagnetic devices under interval uncertainty," *IEEE Trans. Magn.*, vol. 53, no. 6, pp. 1-4, June 2017.
- [12] C. Jiang, X. Han, and G. R. Liu, "Optimization of structures with uncertain constraints based on convex model and satisfaction degree of interval," *Computer Methods in Applied Mechanics and Eng.*, vol. 196, no. 49-52, pp. 4791-4800, 2007.
- [13] C. Jiang, J. Zheng, and X. Han, "Probability-interval hybrid uncertainty analysis for structures with both aleatory and epistemic uncertainties: a review," *Structural and Multidisciplinary Optimization*, vol. 57, no. 6, pp. 2485-2502, Jun. 2018.
- [14] J. Wu, Z. Luo, N. Zhang, and Y. Zhang, "A new uncertain analysis method and its application in vehicle dynamics," *Mechanical Systems and Signal Processing*, vols. 50-51, pp. 659-675, Jan. 2015.
- [15] S. Xiao, Y. Li, M. Rotaru, and J. K. Sykulski, "Six sigma quality approach to robust optimization," *IEEE Trans. Magn.*, vol. 51, no. 3, art. 7201304, Mar. 2015.
- [16] P. N. Koch, R. J. Yang, and L. Gu, "Design for six sigma through robust optimization," *Struct. Multidiscip. Optim.*, vol. 26, no. 3/4, pp. 235-248, Feb. 2004.
- [17] J. Wu, Z. Luo, H. Li, and N. Zhang, "A new hybrid uncertainty optimization method for structures using orthogonal series expansion," *Applied Mathematical Modelling*, vol. 45, pp. 474-490, May 2017.
- [18] S. Brisset and P. Brochet, "Analytical model for the optimal design of a brushless DC wheel motor," *COMPEL-The Int. J. for Computation and Mathematics in Electrical and Electronic Eng.*, vol. 24, no. 3, pp. 829-848, 2005.